ACS Catalysis

Letter

Cite This: ACS Catal. 2018, 8, 6006−6011

pubs.acs.org/acscatalysis

Spatial Coordination of Cooperativity in Silica-Supported Cu/TEMPO/Imidazole Catalytic Triad

Prakash Chandra, Alain M. Jonas, and Antony E. Fernandes*

Institute of Condensed Matter and Nanosciences, Université catholique de Louvain, 1348 Louvain-la-Neuve, Belgium

Supporting Information

ABSTRACT: Multifunctional catalysts obtained by the covalent immobilization of discrete molecular species on porous supports represent a unique approach to emulate some of the design principle and performances of enzymes. However, it is decisive in such systems to control the stoichiometry, spatial distribution, and proximity between the grafted catalytic centers to satisfy the chemical and geometrical requirements for cooperativity. Here, we present strategies to optimize the activity of a catalytic triad on mesoporous silica particles in the representative aerobic oxidation of benzyl alcohol and show that, in contrast with the more-traditional mixed-monolayer approach, activity can be amplified by tuning the spatial distribution of the co-catalysts to maximize the probability of full synergistic pairings.

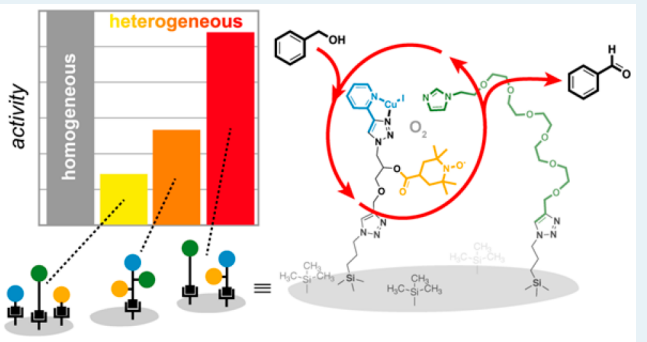

KEYWORDS: *supported catalysis, multifunctional catalysts, cooperativity, CuAAC, alcohol oxidation*

Hybrid multifunctional catalysts that combine two or more molecular active sites on a solid support have emerged as unique heterogeneous catalysts with activity that can compete with, or even surpass that of, the parent homogeneous system, despite intrinsic transport limitations.[1] Beyond catalyst recycling, surface immobilization of cooperative molecular species provides handles to organize, with different degrees of precision, synergistic intermolecular interactions within the multicomponent catalytic system, that are otherwise not easily achievable in higher-entropy homogeneous systems. Hence, in analogy with enzymes where cooperativity results from the perfected preorganization of a handful of chemical functions within a confined space, it is critical to engineer, at the molecular and nanometer scale, the essential features enabling synergistic activation pathways. This encompasses being able to control the spatial distribution, stoichiometry, and time-averaged proximity of active centers on solid surfaces.

Multifunctional silica-supported molecular catalysts are generally prepared by co-condensation,[2] successive grafting,[3] or co-grafting[4] of functional organosilanes. In order to escape the often-arduous synthesis of complex functional silanes, post-synthetic modifications have also been developed in which orthogonally reactive mixed monolayers on silica are reacted with the derivatized catalytic components in a stepwise fashion (Scheme 1a).[5] We recently reported a similar approach in which the cooperative components are covalently immobilized in one step from a monofunctional silica platform (Scheme 1b).[6] In the latter strategy, adjusting the stoichiometric ratio of each component in the grafting solution allows one to control, with high fidelity, the relative surface composition of the solid

Scheme 1. Post-Synthetic Approaches for the Preparation of Multifunctional Supported Molecular Catalysts on Silica

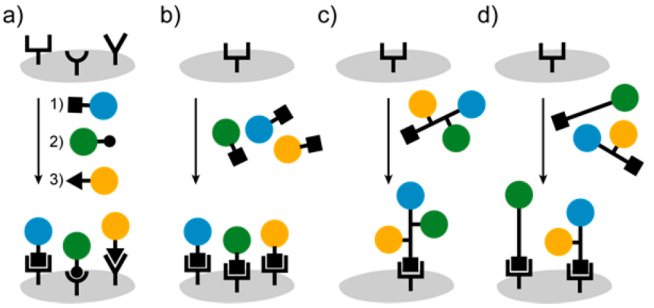

catalyst, which significantly simplifies the precision preparation of multifunctional catalysts.[6,7] This generally requires a very efficient chemistry with wide scope and functional-group tolerance that does not necessitate the use of excess reactants, typically, a "click" chemistry approach.[8] Although often efficient and relatively simple, these approaches do not allow one to control the dispersion (miscible, clustered, segregated) and relative proximity of the active centers on surface, resulting in a distribution of intersite distance and pairing that may dramatically limit the overall efficiency of the catalytic system. Hence, approaches to adjust intersite distance or, more precisely, to preorganize productive intermolecular interactions

Received: April 10, 2018
Revised: May 31, 2018
Published: June 1, 2018

DOI: 10.1021/acscatal.8b01399
ACS Catal. 2018, 8, 6006−6011

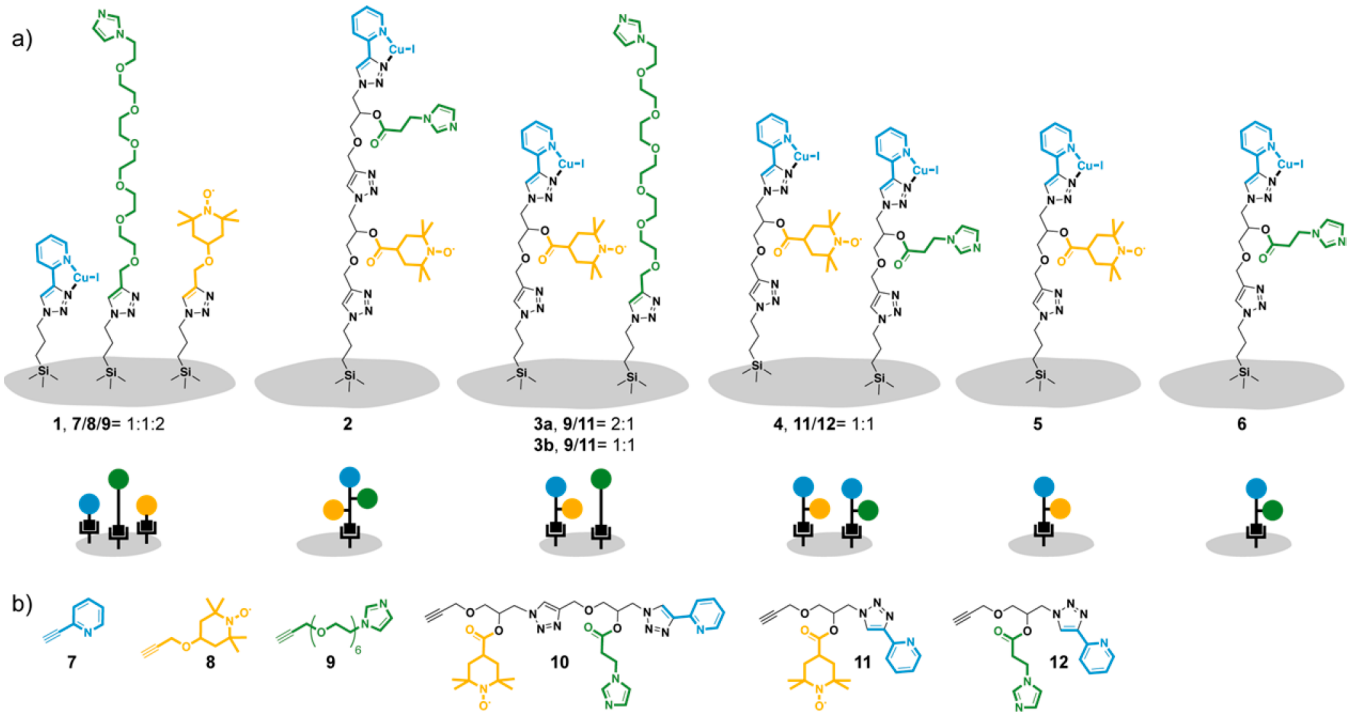

Figure 1. (a) Structure of supported multifunctional catalysts **1**−**6** prepared in one step by CuAAC reaction between azide-silica and alkynes (shown in panel (b)). (b) Structure of monofunctional, bifunctional, and trifunctional alkynes **7**−**12** bearing TEMPO, imidazole, and pyta centers.

between isolated active centers have been developed by engineering grafting density,[9] modulating silica pore size,[3d,10] appending molecular spacers,[6b,10,11] or molecular imprinting.[12]

In another way, arranging the catalytic partners on a single molecule grafted on the surface affords a way to set the proximity between each active center by using the standard arsenal of organic chemistry.[4a,10,13] In a similar approach, we recently described the utilization of short sequence-defined oligomers to adjust and homogenize the spatial distribution of a catalytic triad on surface (Scheme 1c).[14] In this strategy, the catalytic units are orderly distributed along a single oligomeric chain[15] that is subsequently grafted on mesoporous silica particles.

The (bpy)Cu^{I}/TEMPO/NMI catalytic method developed by Stahl and co-workers allows the efficient and selective aerobic oxidation of alcohols to aldehydes and ketones under benign conditions (bpy = 2,2′-bipyridine, TEMPO = 2,2,6,6-tetramethylpiperidine-*N*-oxyl, NMI = *N*-methylimidazole).[16]

In this system, NMI is central for rate acceleration, because it allows reduction of the oxidation potential of the (bpy)Cu^{I} center.[17] The formed (bpy)Cu^{I}(NMI) complex is then easily oxidized by molecular oxygen to form the active oxidizing (bpy)(imidazole)Cu^{II}−$O_2^{\bullet -}$ species,[17,18] this step being turn-over-limiting in the case of activated alcohols, such as benzylic alcohol.[19] On the other hand, the role of TEMPO remains controversial; whereas Stahl and colleagues proposed the formation of a Cu/nitroxyl adduct,[19,20] Rabeah and colleagues postulated that TEMPO is not directly interacting with the Cu center but rather serves for the fixation of the Cu-oxygen radical intermediate.[18]

Following these mechanistic considerations, and the unambiguous, decisive role of imidazole in the catalytic cycle, we prepared supported versions of this catalytic triad focusing on molecularly engineering Cu-imidazole interactions on the surface. In our preliminary design (Scheme 1b), this translated into the incorporation of an ethylene glycol spacer of tailored length to increase the probability of the imidazole site to reach and stay at proximity of the neighboring pyridyltriazole (pyta)Cu^{I} center (catalyst **1**, Figure 1a).[6b] Yet, the random active site distribution in **1** prompted us to investigate the use of precision oligomers to achieve a more uniform distribution (Scheme 1c); cooperative (pyta)Cu^{I}/imidazole interactions operating mainly through interchain interactions as the formation of the (pyta)Cu^{I}(imidazole) complex is intramolecularly less favorable (catalyst **2**, Figure 1a).[14] We reasoned that, in **2**, the synergistic interconnections between the catalytic triad components might similarly be hampered by the limited conformational freedom of the grafted chains.

Here, we present an alternative strategy (Scheme 1d) to preorganize the catalytic triad in order to favor the proximity and productive (geometrically restricted) interactions between the (pyta)Cu^{I} and imidazole sites on surface, together with having the TEMPO locked in close proximity, regardless of whether TEMPO is directly interacting or not with the copper center.

Multifunctional catalysts **1**−**6** (Figure 1a) were prepared in one step by the Cu-catalyzed azide−alkyne cycloaddition (CuAAC) reaction of alkynes **7**−**12** (Figure 1b) with azide-functionalized mesoporous silica particles (see the Supporting Information). Particularly, mixed catalysts **1**, **3a**, **3b**, and **4** were prepared by using stoichiometric mixtures of the corresponding alkyne components (Table S1 in the Supporting Information) in the grafting solution, as previously reported.[6] Using this methodology allows one to control the relative surface composition that reflects the molar ratio of the reactants in the grafting solution.

Thermogravimetric analysis (TGA) allowed quantifying, for each catalyst, the grafting efficiency, with respect to the azide loading, which was overall ≥90% apart for catalysts **2** (75%) and **6** (82%) (see Figure S1 and Table S2 in the Supporting

DOI: 10.1021/acscatal.8b01399
ACS Catal. 2018, 8, 6006−6011

Information). On the other hand, Fourier-transform infrared (FTIR) spectroscopy indicated a decrease of the typical azide band (2100 cm^{-1}) following CuAAC-grafting, together with the apparition of an additional peak at 1715 cm^{-1}, corresponding to ester C═O vibrations in catalysts **2**–**6** (Figure S2 in the Supporting Information). X-ray photoelectron spectroscopy (XPS) analysis confirmed the covalent immobilization of the molecular catalysts and the presence of Cu^{I} species (see Figures S3 and S4, as well as Table S3 in the Supporting Information). On the other hand, nitrogen physisorption demonstrated the decrease in the average pore size and surface area, following CuAAC grafting, which confirms the efficient functionalization (Table S4 in the Supporting Information). Finally, inductively coupled plasma–atomic emission spectroscopy (ICP-AES) allowed one to determine the Cu content for each sample (Table S5 in the Supporting Information).

Catalyst **1**,[6b] prepared via a conventional approach (Scheme 1b) from alkynes **7**–**9**, showed good activity in the benchmark aerobic oxidation of benzyl alcohol using a 5 mol % Cu loading (Figure 2).

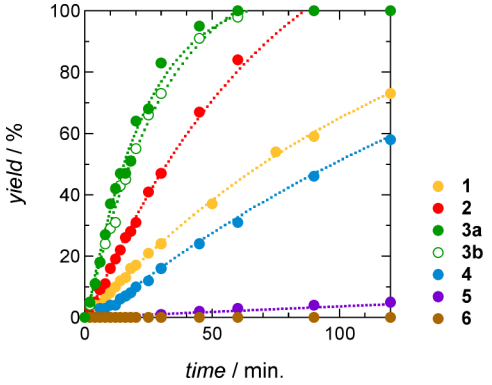

Figure 2. Activity of catalysts **1**–**6** (5 mol % based on Cu) in the aerobic oxidation of benzyl alcohol. Conditions: BnOH (0.2 mmol) in acetonitrile (0.2 M), O_2 bubbling (5.5 mL/min), 60 °C.

Catalyst **2**[14] prepared only from trifunctional oligomer **10** bearing ordered TEMPO, imidazole, and pyta centers on the same molecule, showed accelerated activity (Figure 2), with a 2-fold increase in the initial turnover frequency (TOF), compared to mixed catalyst **1** (see Table 1). This was demonstrated to be associated with the uniform tridimensional distribution of the active centers and the "matched" interchain interactions favoring the formation of the initiating (pyta)Cu^{I}(imidazole) complex.

Table 1. Initial Turnover Frequencies (TOFs)

	Initial TOF (× 10^{-2} min^{-1})		
catalyst	no additive	+ TEMPO	+ NMI
1	16.8	17.8	17.4
2	31.2	32.5	29.2
3a	63.1	47.8	42.7
3b	56.5	52.1	53.0
4	8.7	8.6	24.3
5	0.7	np[a]	5.7
6	0	4.8	np[a]
Bn-pyta + CuI + TEMPO + NMI	69.6		
11 + NMI + CuI	37.4	np[a]	
12 + TEMPO + CuI	4.0		np[a]

[a]Not performed.

In order to enhance the extent of cooperative interactions in supported trimeric catalyst **2**, especially the cooperativity between the TEMPO moiety and the (pyta)Cu^{I}(imidazole) complex (formed through interchain interactions, since intrachain complexation is conformationally disfavored in **2**), mixed catalysts **3a** and **3b** were prepared from imidazole **9** and TEMPO-pyta dimer **11** in a 2:1 and 1:1 ratio, respectively (see Figure 1). Following this design, interchain interactions between the (pyta)Cu^{I} center and imidazole are ensured by means of the hexaethylene glycol spacer (as in **1**), while the TEMPO is locked in the vicinity of the Cu site.

Both **3a** and **3b** outperformed catalysts **1** and **2**, with initial TOFs ca. 4 and 2 times superior, respectively (see Table 1). This confirmed that, in **1**, the random distribution of the triad on the surface does not permit the full pairing of all the active ingredients, whereas in **2**, the ordered distribution, together with restricted conformational freedom in the densely grafted layer, limits synergistic interactions between top and bottom segments of the chains. The mixed distribution in **3a** and **3b** rationally favors the probability of forming the active (pyta)Cu^{I}(imidazole) complex with the TEMPO site in close proximity; this is much less feasible in both **1** and **2**. Biasing the probability of forming the active copper complex by increasing the local surface concentration of the imidazole site in **3a** allows achieving slightly higher activity than **3b**.

Bifunctional catalysts **5** and **6**, missing one active component, showed little or no activity in the oxidation of benzyl alcohol (see Figure 2 and Table 1), demonstrating the importance to have all three components on surface. Adding free *N*-methylimidazole (NMI) or free TEMPO to the incomplete bifunctional heterogeneous catalysts **5** and **6** (see Table 1, as well as Figure S5 in the Supporting Information) allowed catalytic activity to be restored, yet not comparable to that of the supported trifunctional catalysts, probably because the complementary catalytic partner is diluted in the liquid phase, and because of crowding in the grafted layer. The fact that **5** and **6** show similar activity in the presence of free NMI and TEMPO, respectively, confirms that the initiating (pyta)-Cu^{I}(imidazole) complex is mainly formed through intermolecular interactions in **6**, as in **2**. This is also the case for catalyst **4** prepared from an equimolar mixture of TEMPO-pyta **11** and imidazole-pyta **12** dimers (see Figure 2 and Table 1).

Adding free NMI or TEMPO did not yield appreciable improvement of activity with trifunctional catalysts **1**, **2**, **3a**, and **3b** (see Table 1, as well as Figures S6–S9 in the Supporting Information), indicating that the organization of the triad in **1**–**3a**–**3b** cannot be further optimized in their current forms. Rather, adding free TEMPO or NMI to catalyst **3a** showed, instead, a decrease in the reaction rate (see Table 1), suggesting that the addition of free NMI or TEMPO may even disrupt an otherwise already optimal molecular arrangement. However, significantly accelerated activity could be measured with catalyst **4** in the presence of extra NMI (see Table 1, as well as Figure S10 in the Supporting Information), which can be imparted to the fact that (pyta)Cu^{I} is two times more concentrated than imidazole in **4**, together with the incomplete formation of the active Cu complex through interchain interactions, because of random density and distribution of graftings, and because of limitations on molecular motion in dense crowded assemblies.

Catalyst **3a** competed well with the parent homogeneous system consisting of CuI, NMI, TEMPO, and 1-benzyl-4-(2-

DOI: 10.1021/acscatal.8b01399
ACS Catal. 2018, 8, 6006–6011

pyridyl)-1,2,3-triazole ligand (Bn-pyta) (see Figure 3), giving a quantitative conversion in less than 1 h with a similar initial

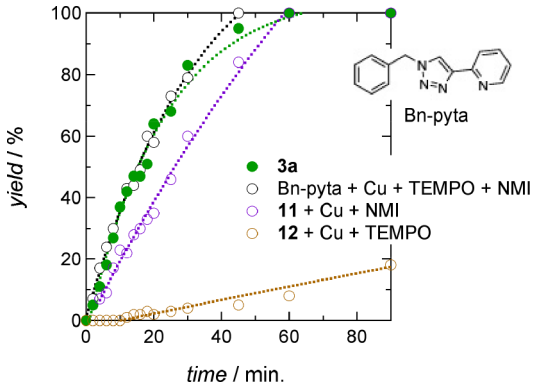

Figure 3. Comparison of **3a** (5 mol % based on Cu) with homogeneous catalytic systems. Conditions: BnOH (0.2 mmol) in acetonitrile (0.2 M), O_2 bubbling (5.5 mL/min), 60 °C. The homogeneous control experiment corresponds to CuI (5 mol %), Bn-pyta (5 mol %), TEMPO (5 mol %), NMI (10 mol %), **11** (5 mol %), and **12** (5 mol %).

TOF (see Table 1). Homogeneous tests employing free dimers **11** and **12**, together with the complementary homogeneous component (NMI and TEMPO, respectively) showed reduced activity, compared to the parent monomeric system (see Figure 3 and Table 1). Especially, imidazole-pyta dimer **12** proved to be 1 order of magnitude slower than TEMPO-pyta **11**, with a TOF similar to its heterogeneous version **6** in the presence of free TEMPO (see Figure S11 in the Supporting Information). This supports the limitation of intramolecular interactions in **6** and **12** for forming the central (pyta)Cu^{I}(imidazole) complex, probably because of conformational hindrances. In **12**, the (pyta)Cu^{I}(imidazole) complex, which is a crucial element of the triad, can mainly form through less-probable intermolecular interactions; in **6**, it is hindered by the restriction of motion in the highly crowded grafted layer.

Catalyst **3a** could easily be filtered and reused for five consecutive recycles (see Figure S12 and Table S6 in the Supporting Information); a maximum turnover number (TON) of ca. 300 was determined (Figure S13 in the Supporting Information). A hot filtration test confirmed the interruption of activity upon removing the catalyst from the reaction mixture, activity that was restored upon readdition of **3a** (Figure S14 in the Supporting Information).

In summary, we demonstrated that cooperativity can be enhanced following rational arrangement of multiple catalytic components on surface. Beyond the traditional approach that consists of the statistical grafting of the individual sites, controlled distribution of the active centers allows one to significantly boost synergistic interactions. Specifically, the later approach presented here increases the probabilities of cooperative interactions of a catalytic triad through interchain and intrachain interactions, in accordance with the postulated reaction mechanism. The formation of a geometrically constrained initiating (pyta)Cu^{I}(imidazole) complex is enabled by flexible interchain interactions, whereas the TEMPO center is held at a favorable distance from the Cu center by being covalently attached to the (pyta)Cu^{I} strand.

Overall, this work provides guidelines for the rational preparation of multifunctional hybrid materials that, so far, has mainly relied in the simple random grafting of individual components on the surface. Controlling the spatial distribution and productive interactions of surface-bound molecules will pave the way to more-efficient catalysts.

■ ASSOCIATED CONTENT

Supporting Information

The Supporting Information is available free of charge on the ACS Publications website at DOI: 10.1021/acscatal.8b01399.

Experimental protocols and characterization data (PDF)

■ AUTHOR INFORMATION

Corresponding Author

*E-mail: antony.fernandes@uclouvain.be.

ORCID

Alain M. Jonas: 0000-0002-4083-0688

Antony E. Fernandes: 0000-0002-7993-2980

Notes

The authors declare no competing financial interest.

■ ACKNOWLEDGMENTS

The authors acknowledge the European Regional Development Fund (ERDF) and Wallonia (Operational Program "Wallonia-2020.EU"), the Belgian Federal Science Policy (IAP P7/05) and the Fonds de la Recherche Scientifique—FNRS and the Fonds Wetenschappelijk Onderzoek under EOS Project No. 30650939 for financial support. Anne Iserentant, Cécile D'Haese, and François Devred are acknowledged for ICP-AES, XPS, and physisorption measurements.

■ REFERENCES

(1) (a) Notestein, J. M.; Katz, A. Enhancing Heterogeneous Catalysis through Cooperative Hybrid Organic−Inorganic Interfaces. *Chem.—Eur. J.* **2006**, *12*, 3954−3965. (b) Motokura, K.; Tada, M.; Iwasawa, Y. Acid−Base Bifunctional Catalytic Surfaces for Nucleophilic Addition Reactions. *Chem.—Asian J.* **2008**, *3*, 1230−1236. (c) Margelefsky, E. L.; Zeidan, R. K.; Davis, M. E. Cooperative Catalysis by Silica-Supported Organic Functional Groups. *Chem. Soc. Rev.* **2008**, *37*, 1118−1126. (d) Shylesh, S.; Thiel, W. R. Bifunctional Acid−Base Cooperativity in Heterogeneous Catalytic Reactions: Advances in Silica Supported Organic Functional Groups. *ChemCatChem* **2011**, *3*, 278−287. (e) Diaz, U.; Brunel, D.; Corma, A. Catalysis Using Multifunctional Organosiliceous Hybrid Materials. *Chem. Soc. Rev.* **2013**, *42*, 4083−4097. (f) Climent, M. J.; Corma, A.; Iborra, S.; Sabater, M. J. Heterogeneous Catalysis for Tandem Reactions. *ACS Catal.* **2014**, *4*, 870−891. (g) Motokura, K. Multifunctional Solid Surfaces for Enhanced Catalysis. *ChemCatChem* **2014**, *6*, 3067−3068.

(2) (a) Huh, S.; Chen, H.-T.; Wiench, J. W.; Pruski, M.; Lin, V. S. Y. Controlling the Selectivity of Competitive Nitroaldol Condensation by Using a Bifunctionalized Mesoporous Silica Nanosphere-Based Catalytic System. *J. Am. Chem. Soc.* **2004**, *126*, 1010−1011. (b) Huh, S.; Chen, H.-T.; Wiench, J. W.; Pruski, M.; Lin, V. S. Y. Cooperative Catalysis by General Acid and Base Bifunctionalized Mesoporous Silica Nanospheres. *Angew. Chem., Int. Ed.* **2005**, *44*, 1826−1830. (c) Zeidan, R. K.; Hwang, S.-J.; Davis, M. E. Multifunctional Heterogeneous Catalysts: Sba-15-Containing Primary Amines and Sulfonic Acids. *Angew. Chem., Int. Ed.* **2006**, *45*, 6332−6335. (d) Puglisi, A.; Annunziata, R.; Benaglia, M.; Cozzi, F.; Gervasini, A.; Bertacche, V.; Sala, M. C. Hybrid Inorganic-Organic Materials Carrying Tertiary Amine and Thiourea Residues Tethered on Mesoporous Silica Nanoparticles: Synthesis, Characterization, and Co-Operative Catalysis. *Adv. Synth. Catal.* **2009**, *351*, 219−229. (e) Shylesh, S.; Wagner, A.; Seifert, A.; Ernst, S.; Thiel, W. R. Cooperative Acid−Base Effects with Functionalized Mesoporous Silica

DOI: 10.1021/acscatal.8b01399
ACS Catal. 2018, 8, 6006−6011

Nanoparticles: Applications in Carbon−Carbon Bond-Formation Reactions. *Chem.—Eur. J.* **2009**, *15*, 7052−7062.
(3) (a) Sharma, K. K.; Biradar, A. V.; Das, S.; Asefa, T. Bifunctional Mesoporous Silica Catalyst for C−C Bond Forming Tandem Reactions. *Eur. J. Inorg. Chem.* **2011**, *2011*, 3174−3182. (b) Motokura, K.; Ito, Y.; Noda, H.; Miyaji, A.; Yamaguchi, S.; Baba, T. Surface Functionalization for Synergistic Catalysis: Silica−Alumina-Supported Cationic Indium and Organic Base for Cyanoethoxycarbonylation. *ChemPlusChem* **2014**, *79*, 1053−1058. (c) Motokura, K.; Saitoh, K.; Noda, H.; Uemura, Y.; Chun, W.-J.; Miyaji, A.; Yamaguchi, S.; Baba, T. Co-Immobilization of a Palladium−Bisphosphine Complex and Strong Organic Base on a Silica Surface for Heterogeneous Synergistic Catalysis. *ChemCatChem* **2016**, *8*, 331−335. (d) Motokura, K.; Ikeda, M.; Nambo, M.; Chun, W.-J.; Nakajima, K.; Tanaka, S. Concerted Catalysis in Tight Spaces: Palladium-Catalyzed Allylation Reactions Accelerated by Accumulated Active Sites in Mesoporous Silica. *ChemCatChem* **2017**, *9*, 2924−2929.
(4) (a) Margelefsky, E. L.; Zeidan, R. K.; Dufaud, V.; Davis, M. E. Organized Surface Functional Groups: Cooperative Catalysis Via Thiol/Sulfonic Acid Pairing. *J. Am. Chem. Soc.* **2007**, *129*, 13691−13697. (b) Motokura, K.; Tada, M.; Iwasawa, Y. Cooperative Catalysis of Primary and Tertiary Amines Immobilized on Oxide Surfaces for One-Pot C-C Bond Forming Reactions. *Angew. Chem., Int. Ed.* **2008**, *47*, 9230−9235. (c) Noda, H.; Motokura, K.; Miyaji, A.; Baba, T. Heterogeneous Synergistic Catalysis by a Palladium Complex and an Amine on a Silica Surface for Acceleration of the Tsuji−Trost Reaction. *Angew. Chem., Int. Ed.* **2012**, *51*, 8017−8020. (d) Noda, H.; Motokura, K.; Miyaji, A.; Baba, T. Efficient Allylation of Nucleophiles Catalyzed by a Bifunctional Heterogeneous Palladium Complex-Tertiary Amine System. *Adv. Synth. Catal.* **2013**, *355*, 973−980. (e) Deiana, L.; Ghisu, L.; Afewerki, S.; Verho, O.; Johnston, E. V.; Hedin, N.; Bacsik, Z.; Córdova, A. Enantioselective Heterogeneous Synergistic Catalysis for Asymmetric Cascade Transformations. *Adv. Synth. Catal.* **2014**, *356*, 2485−2492. (f) Noda, H.; Motokura, K.; Chun, W.-J.; Miyaji, A.; Yamaguchi, S.; Baba, T. Heterogeneous Double-Activation Catalysis: Rh Complex and Tertiary Amine on the Same Solid Surface for the 1,4-Addition Reaction of Aryl- and Alkylboronic Acids. *Catal. Sci. Technol.* **2015**, *5*, 2714−2727. (g) Biradar, A. V.; Patil, V. S.; Chandra, P.; Doke, D. S.; Asefa, T. A Trifunctional Mesoporous Silica-Based, Highly Active Catalyst for One-Pot, Three-Step Cascade Reactions. *Chem. Commun.* **2015**, *51*, 8496−8499. (h) Noda, H.; Motokura, K.; Wakabayashi, Y.; Sasaki, K.; Tajiri, H.; Miyaji, A.; Yamaguchi, S.; Baba, T. Direct Estimation of the Surface Location of Immobilized Functional Groups for Concerted Catalysis Using a Probe Molecule. *Chem.—Eur. J.* **2016**, *22*, 5113−5117. (i) Motokura, K.; Maeda, K.; Chun, W.-J. SiO_2-Supported Rh Catalyst for Efficient Hydrosilylation of Olefins Improved by Simultaneously Immobilized Tertiary Amines. *ACS Catal.* **2017**, *7*, 4637−4641.
(5) (a) Azam, M. S.; Fenwick, S. L.; Gibbs-Davis, J. M. Orthogonally Reactive Sams as a General Platform for Bifunctional Silica Surfaces. *Langmuir* **2011**, *27*, 741−750. (b) Dickschat, A. T.; Behrends, F.; Bühner, M.; Ren, J.; Weiß, M.; Eckert, H.; Studer, A. Preparation of Bifunctional Mesoporous Silica Nanoparticles by Orthogonal Click Reactions and Their Application in Cooperative Catalysis. *Chem.—Eur. J.* **2012**, *18*, 16689−16697. (c) Dickschat, A. T.; Surmiak, S.; Studer, A. Pd Immobilized in Mesoporous Silica Particles as Recyclable Catalysts for Suzuki−Miyaura Coupling: Cooperative Effects Exerted by Co-Immobilized Amine Functionalities. *Synlett* **2013**, *24*, 1523−1528. (d) Dickschat, A. T.; Behrends, F.; Surmiak, S.; Weiss, M.; Eckert, H.; Studer, A. Bifunctional Mesoporous Silica Nanoparticles as Cooperative Catalysts for the Tsuji-Trost Reaction - Tuning the Reactivity of Silica Nanoparticles. *Chem. Commun.* **2013**, *49*, 2195−2197.
(6) (a) Fernandes, A. E.; Riant, O.; Jonas, A. M.; Jensen, K. F. One "Click" to Controlled Bifunctional Supported Catalysts for the Cu/Tempo-Catalyzed Aerobic Oxidation of Alcohols. *RSC Adv.* **2016**, *6*, 36602−36605. (b) Fernandes, A. E.; Riant, O.; Jensen, K. F.; Jonas, A. M. Molecular Engineering of Trifunctional Supported Catalysts for the Aerobic Oxidation of Alcohols. *Angew. Chem., Int. Ed.* **2016**, *55*, 11044−11048.
(7) (a) Tuci, G.; Vinattieri, C.; Luconi, L.; Ceppatelli, M.; Cicchi, S.; Brandi, A.; Filippi, J.; Melucci, M.; Giambastiani, G. "Click" on Tubes: A Versatile Approach Towards Multimodal Functionalization of Swcnts. *Chem.—Eur. J.* **2012**, *18*, 8454−8463. (b) Tuci, G.; Rossin, A.; Xu, X.; Ranocchiari, M.; van Bokhoven, J. A.; Luconi, L.; Manet, I.; Melucci, M.; Giambastiani, G. "Click" on Mofs: A Versatile Tool for the Multimodal Derivatization of N3-Decorated Metal Organic Frameworks. *Chem. Mater.* **2013**, *25*, 2297−2308.
(8) Fernandes, A. E.; Jonas, A. M.; Riant, O. Application of Cuaac for the Covalent Immobilization of Homogeneous Catalysts. *Tetrahedron* **2014**, *70*, 1709−1731.
(9) (a) McKittrick, M. W.; Jones, C. W. Toward Single-Site Functional Materialspreparation of Amine-Functionalized Surfaces Exhibiting Site-Isolated Behavior. *Chem. Mater.* **2003**, *15*, 1132−1139. (b) McKittrick, M. W.; Jones, C. W. Modulating the Reactivity of an Organometallic Catalyst Via Immobilization on a Spatially Patterned Silica Surface. *Chem. Mater.* **2005**, *17*, 4758−4761. (c) Terry, T. J.; Stack, T. D. P. Covalent Heterogenization of a Discrete Mn(Ii) Bis-Phen Complex by a Metal-Template/Metal-Exchange Method: An Epoxidation Catalyst with Enhanced Reactivity. *J. Am. Chem. Soc.* **2008**, *130*, 4945−4953. (d) Nakazawa, J.; Stack, T. D. P. Controlled Loadings in a Mesoporous Material: Click-on Silica. *J. Am. Chem. Soc.* **2008**, *130*, 14360−14361. (e) Nakazawa, J.; Smith, B. J.; Stack, T. D. P. Discrete Complexes Immobilized onto Click-Sba-15 Silica: Controllable Loadings and the Impact of Surface Coverage on Catalysis. *J. Am. Chem. Soc.* **2012**, *134*, 2750−2759. (f) Nakazawa, J.; Hori, T.; Stack, T. D. P.; Hikichi, S. Alkane Oxidation by an Immobilized Nickel Complex Catalyst: Structural and Reactivity Differences Induced by Surface-Ligand Density on Mesoporous Silica. *Chem.—Asian J.* **2013**, *8*, 1191−1199. (g) Smith, B. J.; Hernández Gallegos, P. A.; Butsch, K.; Stack, T. D. P. Metal Complex Assembly Controlled by Surface Ligand Distribution on Mesoporous Silica: Quantification Using Refractive Index Matching and Impact on Catalysis. *J. Catal.* **2016**, *335*, 197−203.
(10) Brunelli, N. A.; Jones, C. W. Tuning Acid−Base Cooperativity to Create Next Generation Silica-Supported Organocatalysts. *J. Catal.* **2013**, *308*, 60−72.
(11) Brunelli, N. A.; Didas, S. A.; Venkatasubbaiah, K.; Jones, C. W. Tuning Cooperativity by Controlling the Linker Length of Silica-Supported Amines in Catalysis and CO_2 Capture. *J. Am. Chem. Soc.* **2012**, *134*, 13950−13953.
(12) (a) Katz, A.; Davis, M. E. Molecular Imprinting of Bulk, Microporous Silica. *Nature* **2000**, *403*, 286. (b) Dufaud, V.; Davis, M. E. Design of Heterogeneous Catalysts Via Multiple Active Site Positioning in Organic−Inorganic Hybrid Materials. *J. Am. Chem. Soc.* **2003**, *125*, 9403−9413. (c) Bass, J. D.; Katz, A. Bifunctional Surface Imprinting of Silica: Thermolytic Synthesis and Characterization of Discrete Thiol−Amine Functional Group Pairs. *Chem. Mater.* **2006**, *18*, 1611−1620. (d) Margelefsky, E. L.; Bendjériou, A.; Zeidan, R. K.; Dufaud, V.; Davis, M. E. Nanoscale Organization of Thiol and Arylsulfonic Acid on Silica Leads to a Highly Active and Selective Bifunctional, Heterogeneous Catalyst. *J. Am. Chem. Soc.* **2008**, *130*, 13442−13449. (e) Peng, Y.; Wang, J.; Long, J.; Liu, G. Controllable Acid-Base Bifunctionalized Mesoporous Silica: Highly Efficient Catalyst for Solvent-Free Knoevenagel Condensation Reaction. *Catal. Commun.* **2011**, *15*, 10−14.
(13) (a) Yu, X.; Yu, X.; Wu, S.; Liu, B.; Liu, H.; Guan, J.; Kan, Q. The Effect of the Distance between Acidic Site and Basic Site Immobilized on Mesoporous Solid on the Activity in Catalyzing Aldol Condensation. *J. Solid State Chem.* **2011**, *184*, 289−295. (b) Lauwaert, J.; Moschetta, E. G.; Van Der Voort, P.; Thybaut, J. W.; Jones, C. W.; Marin, G. B. Spatial Arrangement and Acid Strength Effects on Acid−Base Cooperatively Catalyzed Aldol Condensation on Aminosilica Materials. *J. Catal.* **2015**, *325*, 19−25.
(14) Chandra, P.; Jonas, A. M.; Fernandes, A. E. Sequence and Surface Confinement Direct Cooperativity in Catalytic Precision Oligomers. *J. Am. Chem. Soc.* **2018**, *140*, 5179−5184.

DOI: 10.1021/acscatal.8b01399
ACS Catal. 2018, 8, 6006−6011

(15) (a) Liu, X.; Xia, Q.; Zhang, Y.; Chen, C.; Chen, W. Cu-Nhc-Tempo Catalyzed Aerobic Oxidation of Primary Alcohols to Aldehydes. *J. Org. Chem.* **2013**, *78*, 8531−8536. (b) Prathap, K. J.; Maayan, G. Metallopeptoids as Efficient Biomimetic Catalysts. *Chem. Commun.* **2015**, *51*, 11096−11099. (c) Kinghorn, M. J.; Valdivia-Berroeta, G. A.; Chantry, D. R.; Smith, M. S.; Ence, C. C.; Draper, S. R. E.; Duval, J. S.; Masino, B. M.; Cahoon, S. B.; Flansburg, R. R.; Conder, C. J.; Price, J. L.; Michaelis, D. J. Proximity-Induced Reactivity and Product Selectivity with a Rationally Designed Bifunctional Peptide Catalyst. *ACS Catal.* **2017**, *7*, 7704−7708.

(16) (a) Hoover, J. M.; Stahl, S. S. Highly Practical Copper(I)/Tempo Catalyst System for Chemoselective Aerobic Oxidation of Primary Alcohols. *J. Am. Chem. Soc.* **2011**, *133*, 16901−16910. (b) Hoover, J. M.; Steves, J. E.; Stahl, S. S. Copper(I)/Tempo-Catalyzed Aerobic Oxidation of Primary Alcohols to Aldehydes with Ambient Air. *Nat. Protoc.* **2012**, *7*, 1161−1166.

(17) Hoover, J. M.; Ryland, B. L.; Stahl, S. S. Mechanism of Copper(I)/Tempo-Catalyzed Aerobic Alcohol Oxidation. *J. Am. Chem. Soc.* **2013**, *135*, 2357−2367.

(18) Rabeah, J.; Bentrup, U.; Stosser, R.; Bruckner, A. Selective Alcohol Oxidation by a Copper Tempo Catalyst: Mechanistic Insights by Simultaneously Coupled Operando EPR/UV-Vis/ATR-IR Spectroscopy. *Angew. Chem., Int. Ed.* **2015**, *54*, 11791−11794.

(19) Ryland, B. L.; McCann, S. D.; Brunold, T. C.; Stahl, S. S. Mechanism of Alcohol Oxidation Mediated by Copper(Ii) and Nitroxyl Radicals. *J. Am. Chem. Soc.* **2014**, *136*, 12166−12173.

(20) Walroth, R. C.; Miles, K. C.; Lukens, J. T.; MacMillan, S. N.; Stahl, S. S.; Lancaster, K. M. Electronic Structural Analysis of Copper(Ii)-Tempo/Abno Complexes Provides Evidence for Copper-(I)-Oxoammonium Character. *J. Am. Chem. Soc.* **2017**, *139*, 13507−13517.

DOI: 10.1021/acscatal.8b01399
ACS Catal. 2018, 8, 6006−6011